Towards enhanced stability of human stance with a supernumerary robotic tail

Sajeeva Abeywardena[1] and Ildar Farkhatdinov[2,3] .

***Abstract*—Neural control is paramount in maintaining upright stance of a human; however, the associated time delay affects stability. In the design and control of wearable robots to augment human stance, the neural delay dynamics are often overly simplified or ignored leading to over specified systems. In this letter, the neural delay dynamics of human stance are modelled and embedded in the control of a supernumerary robotic tail to augment human balance. The actuation, geometric and inertial parameters of the tail are examined. Through simulations it was shown that by incorporating the delay dynamics, the tail specification can be greatly reduced. Further, it is shown that robustness of stance is significantly enhanced with a supernumerary tail and that there is positive impact on muscle fatigue.**

***Index Terms*—Wearable Robotics; Human Performance Augmentation; Physical Human-Robot Interaction**

I. Introduction

Human stance has a narrow range of stability due to the location of the centre of mass (CoM) with respect to the relatively small base of support (BoS) provided by the feet. With the mechanical torque created by extensor-flexor muscles in lower limbs found to be below that of the critical stiffness required to overcome gravitational instability; it is well accepted that a neural control element based on vestibular, visual and somatic function accounts for the remaining balance control to maintain upright stance [1]–[3]. However, there is an inherent delay associated with neural control function. Coupled with muscle fatigue, external disturbances and a small base of support; a loss of balance can thus be readily encountered by humans in every day scenarios.

Recent statistics have shown that there are over 684 000 fall related deaths and a further 172 million falls that result in either short or long term disability a year, with those at greatest risk being industrial workers and the ageing population [4]. Enhanced preventative measures to mitigate fall related injuries beyond safe working protocols and targeted training regimes are thus paramount, with robotic intervention being an attractive avenue. Wearable lower limb exoskeletons have been shown to be effective in balance assistance of the general population [5]–[7]. Due to being attached in parallel with the limbs of the wearer; exoskeletons share the same kinematic properties as the assisted limb but the added mass and footprint can hinder the natural motion capabilities.

Supernumerary robotic limbs are an extension of the natural limbs of a human; hence, they have key characteristics to facilitate augmentation of human balance. In this regard, previous works of supernumerary limbs for balance assistance have focussed on extra robotic legs to increase the BoS during walking gait [8]–[10], increasing comfort and posture in near-ground work [11], and for bracing in assembly and overhead tasks to increase the support polygon and reduce muscular loads [12], [13]. Increasing the BoS improves the stability of balance as force is distributed through the ground via more contact points. However, this comes at the cost of increasing the overall footprint of the human which could be an issue due to environmental workspace constraints. Posterior mounted systems such as wearable control moment gyroscopes [14] and supernumerary robotic tails (SRTs) [15] augment balance without increasing BoS. However, these systems add a significant 10-16 kg of mass and inertia to the human body.

The design of wearable robots to augment human performance must carefully consider biomechanical implications and the inherent capabilities of human control. An extra 10 kg at the pelvis can be detrimental to natural human motion [16]; thus minimising mass and inertia in wearable robot design is paramount. However, conflicts arise between desired characteristics and the actual required actuation, geometric and inertial parameters to achieve the specified task. In the realm of balance augmentation, one cause of these issues arises in modelling; namely, simplification or neglect of the neuromechanical delay in design and control due to complexity in the associated mathematics. This leads to systems with over-specified characteristics. Coupled to this is a recent study showing that reactive torques of exoskeletons that augment upright stance need to act faster than human physiology [7]. Efforts to increase response times and power of actuators could achieve this; however, this invariably yields increased reaction torques that are detrimentally applied to the human body. Hence, assistive torques of wearable robots should be informed by predictive estimates of future human state dynamics which depend on mechanical and neural factors.

In this letter; the actuator, geometric and inertial parameters

Manuscript received: March 15, 2023; Revised June 15, 2023; Accepted July 17, 2023. This paper was recommended for publication by Editor Aniket Bera upon evaluation of the Associate Editor and Reviewers' comments. This work was supported by the UK Research and Innovation, Engineering and Physical Sciences Research Council under grant EP/T027746/1 'Automatic Posture and Balance Support for Supernumerary Robotic Limbs'. The authors sincerely thank Professor Etienne Burdet, Radhika Gudipati, Richard Walker and Zaheer Osman for valuable discussions on supernumerary robotic limbs and project support.

[1]S. Abeywardena is with the School of Electronic Engineering and Computer Science, Queen Mary University of London, United Kingdom s.abeywardena@qmul.ac.uk

[2]I. Farkhatdinov is with the School of Engineering and Material Science, Queen Mary University of London, United Kingdom; and [3]Department of Bioengineering, Imperial College of Science, Technology and Medicine, London, United Kingdom i.farkhatdinov@qmul.ac.uk.

Digitial Object Identifier (DOI): see top of this page.

required for a two-degrees-of-freedom (dof) revolute robotic tail to augment human balance with neural delay dynamics incorporated is examined. The organisation is as follows; pertinent background is provided in Section II, the control framework presented in Section III, simulation results discussed in Section IV and the major outcomes for physical human-robot interaction (pHRI) highlighted in Section V.

II. Background

A. System Description

A two-dof tail with revolute joints and serial structure mounted at the height of a wearer's CoM is proposed to augment human balance; where the structure and parameters are illustrated in Fig. 1. Joint variables q_1, q_2 and q_3 and frames are assigned to represent the angle of the passive ankle and two active tail joints respectively. The segments of the tail have link mass distributed at their respective midpoints, i.e. $I_i = \frac{1}{12} m_i {l_i}^2$, with the mass distribution that allows for the tail CoM to be near q_3 obeying

$$m_i = \frac{l_j m_t}{l_i + l_j} \qquad m_j = \frac{l_i m_t}{l_i + l_j} \tag{1}$$

for $(i, j) = (t1, t2)$.

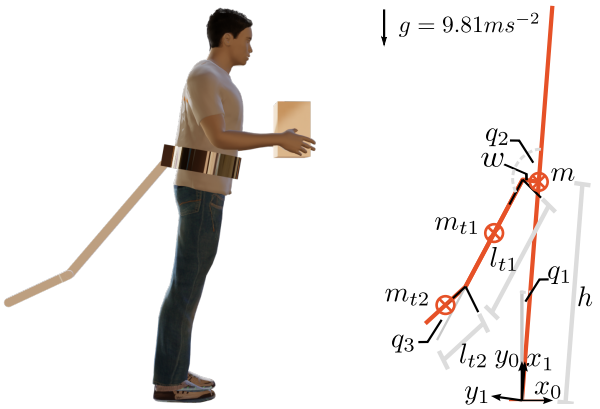

Fig. 1: A supernumerary tail aims to prevent a user from falling when their CoM exceeds the BoS ($\otimes$ represent CoMs)

B. Theoretical Model

The dynamic model of the human-tail system in terms of n_q generalised joint co-ordinates $\mathbf{q}$ is

$$\ddot{\mathbf{q}} = \mathbf{M}(\mathbf{q})\left(-\mathbf{C}(\mathbf{q}, \dot{\mathbf{q}})\,\dot{\mathbf{q}} - \mathbf{g}(\mathbf{q}) + \mathbf{S}\mathbf{u} + \mathbf{u}_p\right) \tag{2}$$

where $\mathbf{M}$ and $\mathbf{C}$ are the $n_q \times n_q$ generalised inertia and centripetal/Coriolis matrices respectively; $\mathbf{g}$ $(n_q \times 1)$, $\mathbf{u}$ $(m \times 1)$ and $\mathbf{u}_p$ $(n_q \times 1)$ vectors of generalised gravity forces, active and passive inputs; and $\mathbf{S}$ an $n_q \times m$ matrix that selects how the m inputs actively alter the n_q joints motion.

Equation (2) is a set of non-linear second-order ordinary differential equations (ODEs). These can be transformed into a system of first order ODEs by defining the state vector $\mathbf{x} = \left[\mathbf{q}^T, \dot{\mathbf{q}}^T\right]^T$. Due to the non-linearity of the system, control design can be complex. However, if only a sub-workspace is of operational interest (i.e. upright human stance), the dynamics

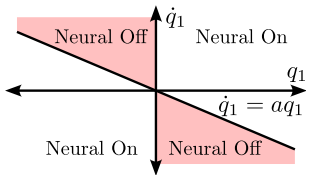

Fig. 2: The intermittent control surfaces of Eq. (4)

can be linearised about a stationary point $(\bar{\mathbf{x}}, \bar{\mathbf{u}})$; allowing for concepts of linear control theory to be applied. As such, the linearised dynamics can be expressed as the system of first order linear ODEs,

$$\dot{\mathbf{x}}(t) = \mathbf{A}\mathbf{x}(t) + \mathbf{B}\mathbf{u}(t) \tag{3}$$

where $\mathbf{A}$ is the $n \times n$ state matrix and $\mathbf{B}$ the $n \times m$ input matrix; $n = 2n_q$ and m is the number of active inputs.

C. Human Control Inputs

The single inverted pendulum (SIP) model accurately represents human stance, with the ankle being the rotational joint [3]. As is well known, the SIP is inherently unstable. For balance, mechanical stiffness at the ankle created by flexor-extensor muscles is insufficient to counteract gravitational instability with delayed neural control providing complementary stabilisation [1]–[3]. Utilising power spectral density analysis of biological sway showed that an intermittent switching controller bests represents the physiology of human neural control stabilisation of upright posture [2]. The fixed point associated with the dynamical equation of the SIP is a saddle point, i.e. the solution to Eq. (2) = 0 and related to the upright equilibrium. This corresponds to a point that can be attracted to a stable or unstable manifold dependent on the flow of the vector field determined by the relationship of angle q_1 and velocity $\dot{q}_1$. As such, in [2], the intermittent switching surface in the $q_1 - \dot{q}_1$ plane was defined by the vertical $\dot{q}_1$ axis and a line with negative slope a through the origin as illustrated in Fig. 2. This divides the plane into quadrants where delayed neural control is switched on when the flow is naturally tending towards the unstable manifold to attract it to the stable manifold; and mechanical ankle stiffness suffices for stabilisation when the flow is naturally in the stable manifold (neural off). Mathematically, this is

$$\mathbf{u}_p = \begin{cases} \text{Neural On: } \mathbf{u}_1 + \mathbf{u}_{1\tau} \text{ if } q_{1\tau}\left(\dot{q}_{1\tau} - aq_{1\tau}\right) > 0 \\ \text{Neural Off: } \mathbf{u}_1 \text{ otherwise} \end{cases} \tag{4}$$

$$\mathbf{u}_1 = -k_p q_1 - k_v \dot{q}_1 \tag{5}$$

$$\mathbf{u}_{1\tau} = -\kappa_p q_{1\tau} - \kappa_v \dot{q}_{1\tau} \tag{6}$$

where $\mathbf{u}_1$ is an impedance model of the ankle joint, $\mathbf{u}_{1\tau}$ is the delayed neural control input, $q_{1\tau} = q_1(t - \tau)$ is the delayed generalised coordinate with time delay τ and $a \leq 0$.

D. Delay Differential Equations

Given that the passive inputs $\mathbf{u}_p$ are expressed in terms of the states of the ankle joint, their contribution can be absorbed

into the state matrix $\mathbf{A}$. For the case of the neural controller being switched off, the dynamics abide by the system equation (3). However, with the neural controller on, the associated time delay changes the governing state equation into a delay differential equation (DDE) of form

$$\begin{aligned}\dot{\mathbf{x}}(t) &= \mathbf{A}\mathbf{x}(t) + \mathbf{A}_\tau \mathbf{x}_\tau(t) + \mathbf{B}\mathbf{u}(t) \\ \mathbf{x}(t) &= \boldsymbol{\phi}(t) \quad -\tau \leq t \leq 0\end{aligned} \tag{7}$$

where $\mathbf{A}_\tau$ is the $n \times n$ state delay matrix, $\mathbf{x}_\tau(t) = \mathbf{x}(t-\tau)$ the delayed state vector and $\boldsymbol{\phi}(t)$ the initial condition over the previous delay period. As a consequence, the characteristic equation of the system is the quasi-polynomial

$$s\mathbf{1} - \mathbf{A} - \mathbf{A}_\tau \exp(-s\tau) = 0 \tag{8}$$

which has infinite poles, complicating analysis.

Due to the infinite dimensional nature of Eq. (7), standard solution methodologies of ODEs are not directly applicable. Nevertheless, it is attractive to attempt a conversion of a DDE into an ODE to utilise well developed analysis techniques. In [2], a Taylor series approximation was utilised to convert the delayed terms to finite dimension. However, there is no mathematical basis to such an approximation as it poorly encapsulates the infinite poles of systems with large time delay such as human balance [17]. Spectral time approximations (STA) utilise an irregular grid to characterise an infinite dimensional system [18]. Corresponding to the extremes of the Chebyshev polynomial of the first kind with degree N, Chebyshev collocation points are unevenly spaced on the domain $[-1, 1]$ i.e.

$$t_j = \cos\left(\frac{j\pi}{N}\right) \quad j = 0, 1, \ldots N \tag{9}$$

Given that there are $k = N + 1$ collocation points defined by Eq. (9), the spectral differencing matrix $\mathbb{D}$ is of dimension $k \times k$. Indexing the rows and columns of $\mathbb{D}$ from 0 to N,

$$\begin{aligned}\mathbb{D}_{00} &= \frac{2N^2+1}{6} \quad \mathbb{D}_{NN} = -\frac{2N^2+1}{6} \\ \mathbb{D}_{jj} &= \frac{-t_j}{2\left(1-{t_j}^2\right)} \quad j = 1 \ldots N-1 \\ \mathbb{D}_{ij} &= \frac{c_i\,(-1)^{i+j}}{c_i\,(t_i - t_j)} \quad i \neq j, i, j = 0 \ldots N \\ c_i &= \begin{cases} 2 \text{ for } i = 0, N \\ 1 \text{ otherwise} \end{cases}\end{aligned} \tag{10}$$

Equation (10) is the differentiation operator for one DDE. For n DDEs, the $kn \times kn$ spectral differentiation operator is

$$\mathcal{D} = \mathbb{D} \otimes \mathbf{1}_n \tag{11}$$

where $\mathbf{1}_n$ is the $n \times n$ identity matrix and $\otimes$ denotes the Kronecker product.

Having defined the differentiation operator $\mathcal{D}$, a spectral time approximation to Eq. (7) can be made. Let

$$\mathbf{z}(t) = \begin{bmatrix}\mathbf{z}_1(t) \\ \vdots \\ \mathbf{z}_k(t)\end{bmatrix} = \begin{bmatrix}\mathbf{x}(t) \\ \vdots \\ \mathbf{x}(t-\tau)\end{bmatrix} = \begin{bmatrix}\mathbf{x}(t_0) \\ \vdots \\ \mathbf{x}(t_N)\end{bmatrix}$$

where $\mathbf{z}_i$ is the $n \times 1$ state vector at time t_j (given by Eq. (9)) and $\mathbf{z}$ is the $kn \times 1$ state vector in the period $[0, \tau]$. Then the finite approximation of the DDE (7) is

$$\begin{aligned}\dot{\mathbf{z}}(t) &= \begin{bmatrix}\mathbf{A} & \mathbf{0}_{n\times(k-2)n} & \mathbf{A}_\tau \\ \frac{2}{\tau}\mathcal{D}\,(n+1:kn,:)\end{bmatrix}\mathbf{z}(t) + \begin{bmatrix}\mathbf{B} \\ \mathbf{0}_{(k-1)n\times m}\end{bmatrix}\mathbf{u}(t) \\ \dot{\mathbf{z}}(t) &= \tilde{\mathbf{A}}\mathbf{z}(t) + \tilde{\mathbf{B}}\mathbf{u}(t)\end{aligned} \tag{12}$$

where $\tilde{\mathbf{A}}$ is the Chebyshev spectral state matrix in which the first n rows of $\mathcal{D}$ are replaced by the state equation at the current instance, $\tilde{\mathbf{B}}$ is the $kn \times m$ input matrix, $\mathbf{0}$ are appropriately dimensioned zero matrices and $\frac{2}{\tau}$ scales the collocation points into the interval $[0, \tau]$. Equation (12) is in the form of Eq. (3); hence, techniques of finite ODEs and linear control can be applied. Further, without loss of generality, $\mathbf{x} = \mathbf{z}$ for the remainder of this letter.

III. Control Development

The development of control laws for multi-input, multi-output (MIMO) systems in the form of Eq. (3) are well developed, including pole placement and optimal control. For STA systems of Eq. (12) which are in the same structure as Eq. (3), kn poles spectrally approximate the infinite dimensional system; a number which is too large to intuitively select using pole placement. As such, optimal control techniques are best suited for the MIMO STA systems encountered in this letter. The cost function for optimisation is defined as

$$J = \int_0^{T_p} \mathbf{x}(t)^T \mathbf{Q}\mathbf{x}(t) + \mathbf{u}(t)^T \mathbf{R}\mathbf{u}(t)dt \tag{13}$$

where T_p is the prediction horizon, with $\mathbf{Q}$ and $\mathbf{R}$ weighting matrices on the states and inputs respectively.

Model predictive control (MPC) determines an optimal trajectory of the control input using predictions of the future dynamics of the system with constraints on inputs, outputs and states. This is well suited to the requirements of this study, where actuation limits and constraints on the range of motion are to be enforced. As MPC theory is well developed, the interested reader is directed to Chapters 5-8 of [19] for details on the MPC formulation used in this work.

A. Virtual Constraints

Using MPC to formulate the control; constraints on input, output and state variables can be applied. However, soft constraints on the state and output constraints are employed to prevent conflicts in optimisation. For a supernumerary robotic tail, limits on input levels and tail motion are equally important to facilitate safe pHRI. As such, virtual (rather than soft) constraints formulated via repulsive potential fields are used to prevent collisions of the tail with the human body. Namely, an inverse distance potential field in joint space with damping added on the associated joint's velocity to soften the impact of the repulsive force and maintain stable motion, i.e.

$$u_{r,i} = -b_i\dot{q}_i + \sum_{j=1}^{K} \frac{\mu_j}{(q_i - \hat{q}_j)^3} \tag{14}$$

where b_i is a damping coefficient for joint i, μ_j and $\hat{q}_j$ are respectively constants representing the strength and boundary

of the j-th potential field acting on joint q_i. The total repulsive torque is added directly to the input calculated via MPC for each of the active joints.

B. Stability

Due to the intermittent switching nature of human stance, the control law of the active tail will switch. Whilst stable control laws can be developed using MPC for both the ODE and STA dynamics independently, this does not guarantee that stability is maintained between switching. Further, the presence of constraints on the control input and motion of the tail can also have a consequence on the overall stability of the system. In [2], a Poincare section based on the switching function of Eq. (4) was defined and a Poincare map used to assess stability of quiet stance based on a range of neural control parameters (κ_p, κ_v). The Poincare map considers only a section of flow, and if the map converges to the same point with time it is consider to be stable.

Lyapunov exponents consider the trajectory of infinitesimally close hyperspheres in the phase space of the dynamics. Traditionally utilised to determine chaotic attractors, n Lyapunov exponents exist for a n-dimensional vector field, with the largest quantitatively assessing the convergence/divergence of the system. It is defined as

$$\lambda = \lim_{t\to\infty} \frac{1}{t} \ln\left(\frac{\|\delta\mathbf{x}(t)\|}{\|\delta\mathbf{x}(0)\|}\right) \tag{15}$$

where $\delta\mathbf{x}(t)$ represents the trajectory of the hypersphere. If the largest Lyapunov exponent $\lambda > 0$, the system is unstable.

Calculation of the Lyapunov exponent can be conducted using analytic equations in terms of states of the flow, i.e. Eq. (2), (3), (7) or (12), in conjunction with the variational equation. However, the intermittent switching control and constraints cause discontinuities in flow; hence, calculating Eq. (15) using analytic methods is further complicated. Nevertheless, Wolf's algorithm [20] allows for the Lyapunov exponent to be calculated from a time series and is utilised to quantitatively assess the stability of the human-supernumerary tail systems considered in this letter.

IV. Simulation

A simulation study was conducted to assess the joint actuation, inertial and geometric characteristics of a supernumerary robotic tail to augment human balance. A human of height 1.8 m, CoM h located 0.997 m directly above the ankle joint, mass m of 82.2 kg and inertia of 12.92 kg-m^2 was simulated [21]. In line with the study of [2], ankle mechanical stiffness was set as $k_p = 0.8mgh$ Nm and $k_v = 4$ Nm/s with respect to Eq. (5) (i.e. the ankle muscles compensates 80% of gravitational torque); and neural control parameters of Eq. (6) ranged from 0 to $0.8mgh$ for κ_p and 0 to 60 Nm/s for κ_v. The tail was mounted at the CoM of the human and 0.1 m posterior to the trunk as illustrated in Fig. 1. Three cases of tail mass and geometric parameters were considered, as tabulated in Table I, with the system linearised about the stationary point $[q_1, q_2, q_3] = [0, 150, -20]^\circ$. In [2], an initial angle value of $q_1 = 0.57^\circ$ was utilised. This correlates

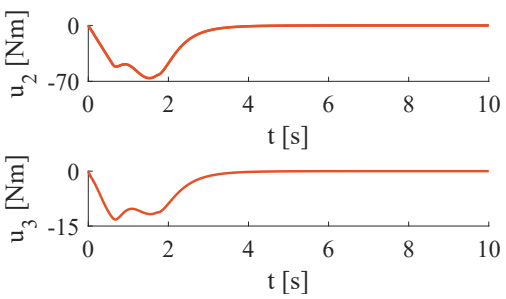

Fig. 3: The baseline torque profiles for q_2 and q_3 with no neural control $(\kappa_p = 0, \kappa_v = 0)$ and Case I parameters

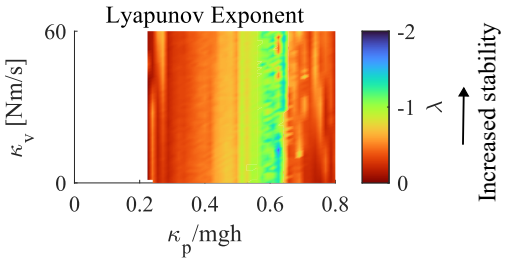

Fig. 4: Lyapunov exponent of quiet standing without assistance from a supernumerary tail

to experimental measurements of physiological human sway to maintain quiet stance. In this work, initial conditions of $\mathbf{x}_0 = [6^\circ, 0, 0, 0, 0, 0]^T$ about the stationary point and the delay history of $\mathbf{0}$ was used, i.e. a disturbance 10 times larger than that of maintained postural sway which pushes the CoM towards exceeding the BoS and potential to topple forward.

TABLE I: The inertial-geometric parameter cases considered in this study which respect Eq. (1).

Case	m_{t1} [kg]	l_{t1} [m]	m_{t2} [kg]	l_{t2} [m]
I	3.33	0.6	6.67	0.3
II	1.67	0.6	3.33	0.3
III	0.83	0.6	1.67	0.3
IV	0.83	0.3	1.67	0.15

The STA model of Eq. (12) with a Chebyshev polynomial of degree $N = 10$ was used to approximate the infinite dimensional DDE. As 6 states represented the finite dimensional system of Eq. (3), the spectral approximation had dimension 66. The DDE required time history up to τ seconds; hence, the neural off control model, was also represented by a 66 dimensional system—with $\mathbf{A}_\tau = \mathbf{0}_{6\times6}$ in Eq. (12)—to allow continuity of the delayed state approximation. MPC laws were designed using the notion of prescribed stability described in Chapter 8 of [19]. In particular, the poles were set to lie to the left of the $s = -0.8$ line, prescribing the dominant poles to have a settling time of 5 s. $\mathbf{Q}$ in Eq. (13) was set to only apply on the current system states for both the ODE and DDE controllers, with weights of 1000 (ODE) and 50 (DDE) used, and $\mathbf{R} = \mathbf{1}_2$ for both.

As a baseline for comparison, the torque required to aug-

ment balance for Case I in Table I without neural control (i.e. $(\kappa_p, \kappa_v) = (0, 0)$) or constraints was simulated and shown in Fig. 3. From this figure, around 67 Nm and 14 Nm of torque are required at the first and second joints of the tail respectively to return the human to upright posture. Using this, joint actuation limits of the tail was set as ± 30 Nm for the simulations that consider delay dynamics. Repulsive potential fields to prevent the tail interfering with the posterior of the human were defined by Eq. (14); with boundaries set at 0 and 180° to the body for both q_2 and q_3. The fields had strengths $\mu_j = \left(\frac{\pi}{180}\right)^3$, and damping gains of 0.5 and 0.05 Nm/s for $\dot{q}_2$ and $\dot{q}_3$ were respectively used, with these values manually tuned to ensure stable motion for Case I parameters at normalised $\kappa_p = 0.3, 0.6, 0.8$ and $\kappa_v = 30$ Nm/s; and maintained throughout. Conservatively, the potential fields became active at 20° and 160°.

A. Stability

An intermittent switching parameter of a = -0.4 was used with the time delay of the neural controller set at $\tau = 0.2$ s which is considered 'challenging' [2], [3]. The Lyapunov exponent was calculated for unassisted quiet standing and shown in Fig. 4. The distribution of λ in this figure matches well with that provided in [2] which utilised Poincare mapping, validating the use of the Lyapunov exponent as a quantitative stability indicator in this letter. In particular, it can be seen that the most stable region (i.e. most negative λ) is in the normalised κ_p = 0.5-0.6 range and as this value heads in either direction, the flow has greater propensity to cross into the unstable region as λ approaches 0. Further, as the mechanical stiffness compensates 80% of gravitational torque, a normalised κ_p of more than 0.2 is required for the neural controller to provide stabilisation of upright stance.

The four cases of inertial and geometric tail parameters tabulated in Table I were simulated for all combinations of neural control parameters κ_p and κ_v stated previously. Figure 5 shows the Lyapunov exponent and maximum required torques for the two joints of the tail; with Case I-IV shown from top to bottom. Examining the Lyapunov exponent in the first column of Fig. 5 and comparing with Fig. 4; evidently a supernumerary tail greatly increases the stability region of neural control parameters. That is, with a tail, even if neural control is diminished ($\kappa_p \leq 0.2$) upright pose can be maintained. Further, the most negative λ (i.e. green region) for unassisted standing is spread throughout with the use of a robotic tail. This indicates, hypothetically, that with a tail less strain could be placed on the neural controller as smaller neural proportional gain κ_p is required to attain comparable 'optimal stability' of unassisted stance. Within the cases, Case II provides the greatest range of neural control parameters with Case IV (lightest and shortest) providing the smallest but larger than unassisted. Further, Case I (heaviest) and Case IV (lightest and shortest) have similar range; indicating a trade off between mass and length of the tail is required in design and importantly that the heaviest solution is not the most optimal. Hence, it is ascertained that a supernumerary tail improves the robustness of quiet stance.

B. Torque

The required maximum tail torques to augment balance are illustrated in columns 2 (q_2) and 3 (q_3) of Fig. 5. Seemingly, when normalised κ_p is in the 0.4-0.6 range, the torques attain their minimums. Further, Case I (heaviest) has the greatest torque requirements for both joints. Similarly, as normalised $\kappa_p \geq 0.6$, the maximum torque requirements for q_2 increase (particularly for Case III and IV). This can be attributed to there being added proportional neural gain in the system, hence the unassisted response is more oscillatory. As a result, larger torque and velocity of the tail potentially results to counteract oscillations and achieve quiet stance. However, this could lead to the tail violating safety constraints with the virtual constraints engaged to push the tail towards a safe region, increasing the required torque. Such phenomena explains interior missing points in Fig. 5 which could be attained by fine tuning potential field parameters.

Similarly, for Case I-III, as normalised $\kappa_p \leq 0.2$, the torque requirements increase. In this situation, proportional neural control is lacking and added torque is required from the tail to attain upright posture. Contrarily, the torque requirements for the second tail joint q_3 is fairly consistent throughout the parameter space for all cases, between 1-8 Nm. Hence, this knowledge can be utilised in the design of a supernumerary tail as the second tail joint has lower actuation requirements than the first. It should be noted that these values are the required torques at the joints, not from an actuator and it is envisaged that a suitable transmission can be designed to achieve the specification. Nevertheless—through modelling the human's inherent neural delay dynamics and irrespective of parameters in Table I—human balance augmentation with a supernumerary tail can be achieved with significantly less torque than the 67 Nm for the baseline case of Fig. 3. This overall leads to a simpler design and safer pHRI.

C. Range of Motion

The range of motion (RoM) of the joints is a metric of interest for use of a robotic tail. The RoM of the three joints for all combinations of κ_p and κ_v are shown in Fig. 6. It can be seen that the RoM of the ankle joint is consistent between all four inertial-geometric parameter combinations, around 7°, indicating that there is a slight overshoot in the response of the ankle before upright stance is achieved. This is expected as the initial disturbance will cause the velocity of the ankle to move in the direction of gravitational instability before the neural control and robotic tail provide stabilisation. For the tail joints, the normalised κ_p range of 0.4-0.6 has a similar and smallest amount of RoM in q_2 which correlates with the joint torque minimisation discussed previously. Hence, it is ascertained that in this region there is symbiotic control action between the neural controller and the tail, i.e. it is the most optimal region. As proportional neural control drops, the RoM of q_2 increases. Given that the stationary point of this joint is 150° and close to a virtual constraint, this indicates a swing backwards to create sufficient momentum to augment balance as κ_p gets smaller. Case I, however, has a RoM of q_2 that is consistent; hence, the extra mass primarily augments balance.

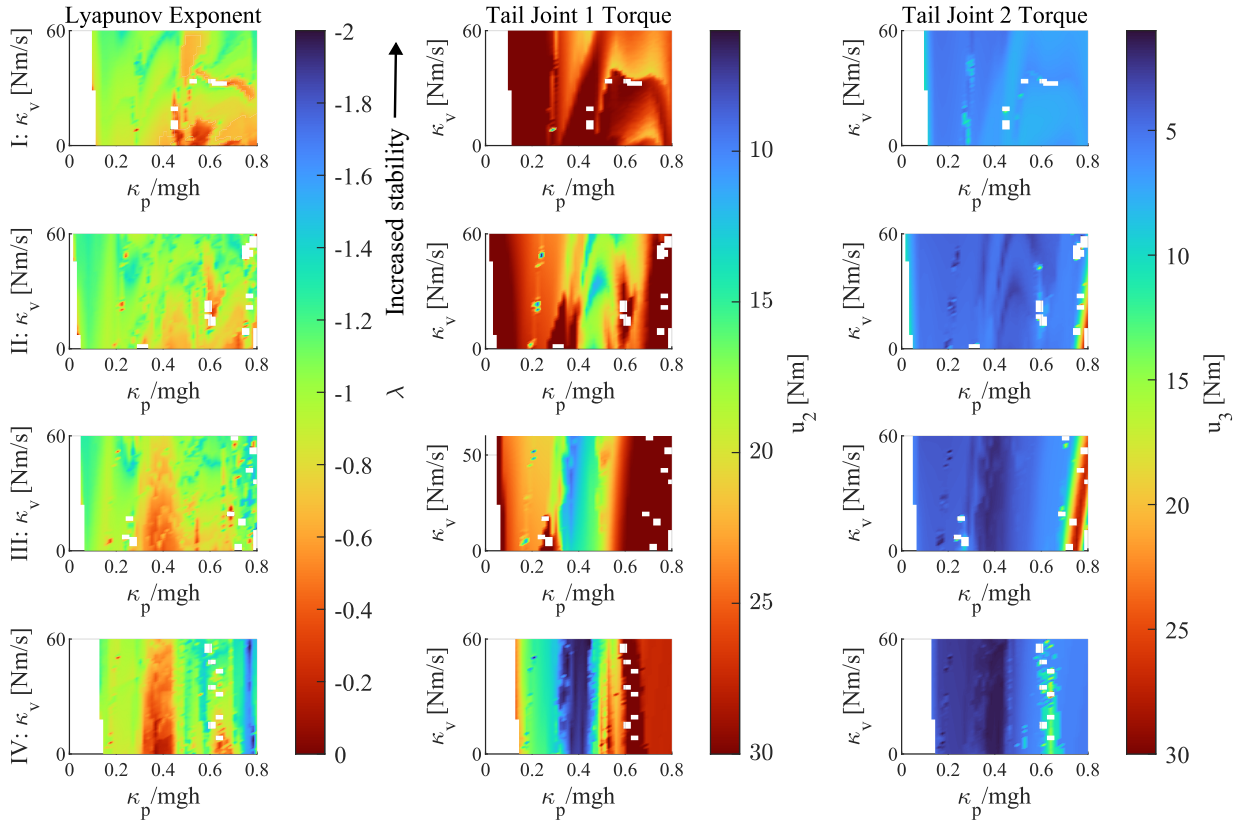

Fig. 5: Comparison of the stability via maximum Lyapunov exponent and joint torque requirements for the four inertial-geometric cases in Table I (Top-bottom: Case I—IV) and range of neural control parameters (κ_p, κ_v)

Within Cases II-IV, Case II (5 kg, 0.9 m) utilises the smallest joint RoM and Case III (2.5 kg, 0.45 m) the greatest. This is particularly evident when investigating the RoM of q_3 for Case III which corresponds to the largest amount of motion. The increase in RoM can be explained through the notion of coupling inertia (off diagonal terms in $\mathbf{M}$ of Eq. (2) that are defined by mass, length and RoM of tail segments) which is critical in creating a reactive torque to augment balance against gravity [22]. Case IV corresponds to the lightest and shortest total tail length considered. As such, the coupling inertia due to mass and length is reduced when compared with the other tails. Further, the added mass in Case I means it has the highest amount of inertia in the tail, hence why it has the smallest RoM. Thus, Case IV utilises larger motion in q_3 to augment balance in the presence of smaller structural inertia. Hence, in supernumerary tail design, coupling inertia is paramount; requiring a balance between mass, length and joint RoM.

D. Time Response

The time response of the joints for the three considered cases in Table I along with the unassisted case are shown in Fig. 7. Three κ_p levels were considered; 0.3, 0.5 and 0.8 with κ_v fixed at 24 Nm/s. For all levels of κ_p, upright stance is achieved in the desired 5 s, with intermittent switching noticeable from the profiles. Comparing to the unassisted case, this is a great improvement for κ_p = 0.3 and 0.8. As can be seen, for κ_p = 0.3 the response is sluggish and potentially over-damped whilst for κ_p = 0.8 the ankle profile is highly oscillatory and significantly under-damped, potentially indicative of neurological conditions that induce tremors. For κ_p = 0.5, there is no discernible difference between the response with and without tail, matching with the notion that in this region the neural controller and tail act symbiotically. These results match with the Lyapunov exponent distributions in Fig. 5 compared to Fig. 4; that is, the more negative λ associated with more stable flow is indicative of quicker response to upright pose with a tail. Further, the response of the tail joints matches with the RoM in Fig. 6. Of particular note is the extra motion of q_3 in Case IV for κ_p = 0.5. This is potentially due to smaller RoM of q_2 and compensating lower structural inertia.

The passive mechanical ankle torque is also illustrated in Fig. 7. For κ_p = 0.3 and 0.8, the tail responses settle much quicker than unassisted. As the initial ankle torque is the same for all cases, this will result in less ankle energy expenditure with a tail. However, the caveat is Case I (10 kg tail) for $\kappa_p = 0.3, 0.5$ which has the longest rise time and overshoot, i.e. slowest initial rate of change. Thus, there is an initial increase in ankle torque and overall energy use compared to the lighter tails that achieve quicker response. However, Case I has similar response to these tails when $\kappa_p = 0.8$, i.e. the added inertia is beneficial in damping the natural oscillations. Hence, a supernumerary tail enhances stability of stance from a neural perspective and has potential to reduce muscle fatigue.

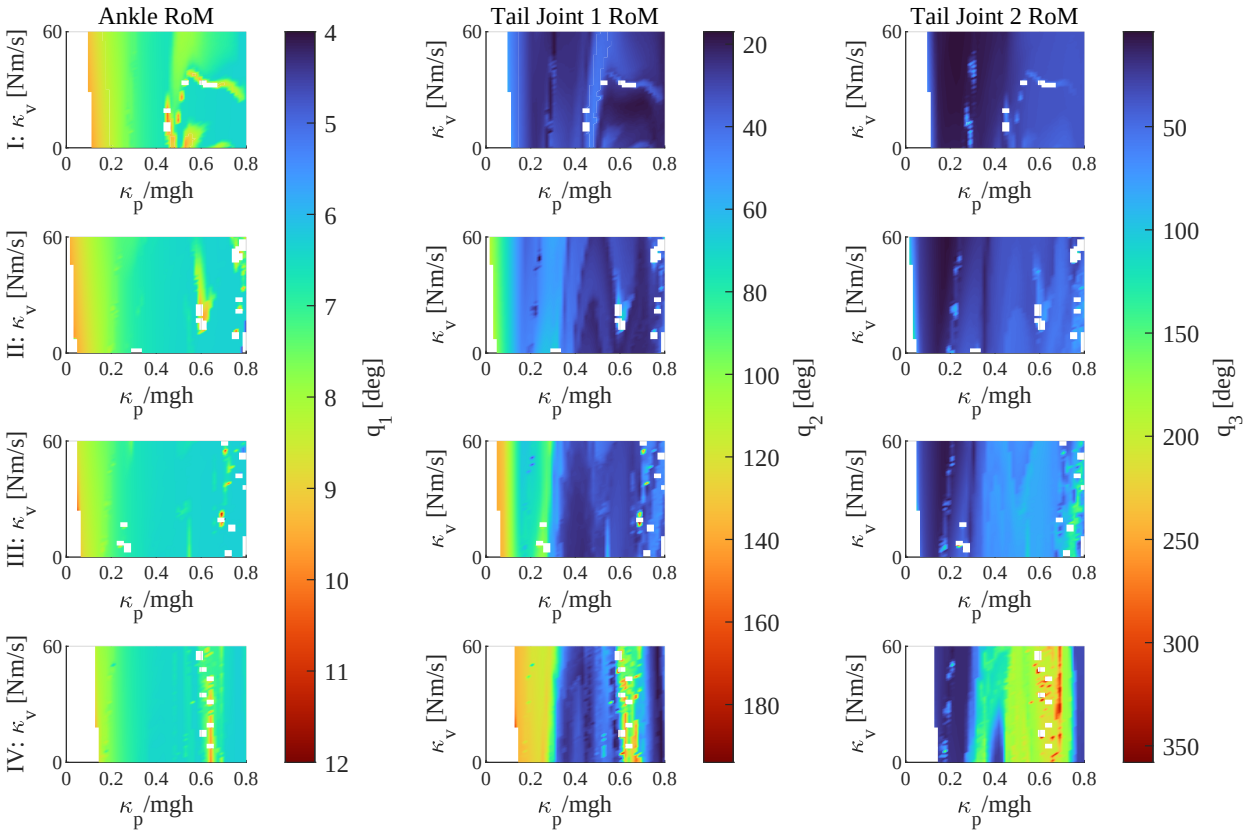

Fig. 6: The range of motion of the ankle and tail joints required to provide stable balance augmentation for the four inertial-geometric cases in Table I (Top-bottom: Case I—IV) and range of neural control parameters (κ_p, κ_v)

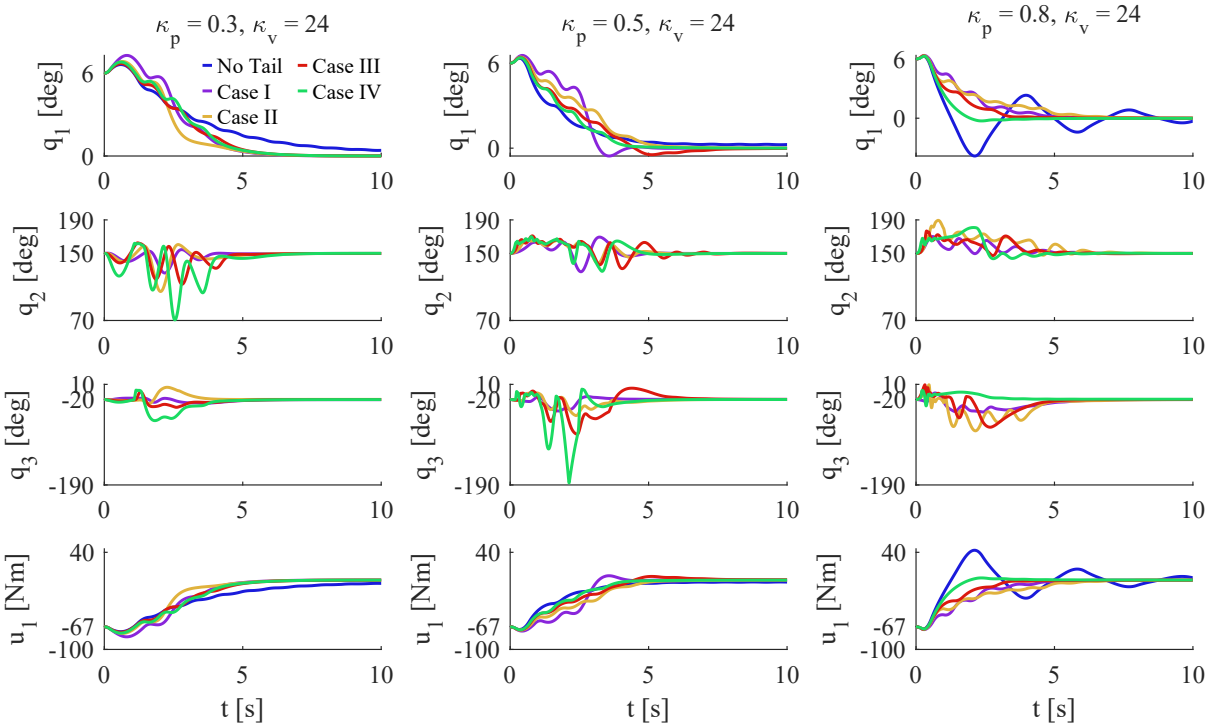

Fig. 7: Time response with and without tail (videos available as supplemental material). The ankle and tail joint angles are shown in rows 1-3 and ankle mechanical torque in row 4 for various (κ_p, κ_v). Tail parameters are as tabulated in Table I.

V. Conclusion and Future Work

Evidentially, this letter has shown the promising characteristics that a two-dof supernumerary tail can have on enhancing human stance. The inertial and geometric characteristics of the tail very much depend on the level of assistance required for the potential application; in a warehouse situation where a tail could be used as a counter balance in load handling and minimise added postural sway, assuming a wearer has no underlying issues affecting maintaining stance, a lighter and shorter tail may suffice to reduce neural control requirements. That is, the results show a tail has the ability to maintain stance in a stable and quick fashion with lower neural/mental requirements compared to unassisted. Subsequently, this could improve mental alertness and improve daily productivity. If there are underlying neurological issues of the wearer, a heavier and/or longer tail would be more beneficial to increase the coupling inertia; however, this comes at the potential cost of added actuation requirements to augment stance in a timely manner.

The notion of measuring and augmenting neural control function is difficult to quantify. Overall stability of stance could be evaluated by intermittently calculating the Lyapunov exponent related to measured ankle states and used as an adaptive control indicator in conjunction with Fig. 4. Further, long term plasticity effects would need to be assessed to examine if the use of a supernumerary tail has an effect on the neural level of control as hypothesised above. In particular, if a potential wearer develops an over reliance on the augmentation assistance from a tail and struggles to adjust to standing without.

Supernumerary robotic tails are still in their infancy, with this work determining if such technology is useful for human stance. Compared with existing augmentation and support technology such as exoskeletons and portable harnesses, supernumerary tails do not directly interfere with the natural joints and limbs; however, a concerted user study comparison is required. Further, the impact on the lumbar spine and other areas must also be examined in the future. Added investigation into incorporating the extra limbs into every day motion such a sitting, bending and lifting is still required. The impact on locomotion with a tail is pertinent; particularly how to synchronise the added appendage with the periodicity of stable bipedal gait. However, this requires the current SIP model of stance to be expanded into non-linear multi-dof models appropriate for locomotion, bending and sitting with delayed neural control embedded. Nevertheless, this letter showed that the use of mathematical modelling techniques of neural-mechanical control of a human leads to a reduction in the requirements of actuator, geometric and inertial parameters for wearable robot design. For the field of pHRI this is significant as it allows for the development of correctly specified wearable robots, and potential minimisation of disturbances to the human body.

References

[1] R. J. Peterka, "Postural control model interpretation of stabilogram diffusion analysis," *Biological Cybernetics*, vol. 82, pp. 335–343, 2000.

[2] Y. Asai, Y. Tasaka, K. Nomura, T. Nomura, M. Casadio, and P. Morasso, "A model of postural control in quiet standing: Robust compensation of delay-induced instability using intermittent activation of feedback control," *PLOS ONE*, vol. 4, no. 7, pp. 1–14, 07 2009.

[3] P. Morasso, A. Cherif, and J. Zenzeri, "Quiet standing: The single inverted pendulum model is not so bad after all," *PLOS ONE*, vol. 14, no. 3, pp. 1–20, 2019.

[4] World Health Organisation, "Step safely: strategies for preventing and managing falls across the life course," 2021.

[5] V. Monaco, P. Tropea, F. Aprigliano, D. Martelli, A. Parri, M. Cortese, R. Molino-Lova, N. Vitiello, and S. Micera, "An ecologically-controlled exoskeleton can improve balance recovery after slippage," *Scientific Reports*, vol. 7, p. 46721, 9 2017.

[6] I. Farkhatdinov, J. Ebert, G. van Oort, M. Vlutters, E. van Asseldonk, and E. Burdet, "Assisting human balance in standing with a robotic exoskeleton," *IEEE Robotics and Automation Letters*, vol. 4, no. 2, pp. 414–421, 2019.

[7] O. N. Beck, M. K. Shepherd, R. Rastogi, G. Martino, L. H. Ting, and G. S. Sawicki, "Exoskeletons need to react faster than physiological responses to improve standing balance," *Science Robotics*, vol. 8, no. 75, p. eadf1080, 2023.

[8] M. Hao, J. Zhang, K. Chen, H. Asada, and C. Fu, "Supernumerary Robotic Limbs to Assist Human Walking With Load Carriage," *Journal of Mechanisms and Robotics*, vol. 12, no. 6, 07 2020, 061014.

[9] C. Khazoom, P. Caillouette, A. Girard, and J.-S. Plante, "A supernumerary robotic leg powered by magnetorheological actuators to assist human locomotion," *IEEE Robotics and Automation Letters*, vol. 5, no. 4, pp. 5143–5150, 2020.

[10] D. J. Gonzalez and H. H. Asada, "Hybrid open-loop closed-loop control of coupled human-robot balance during assisted stance transition with extra robotic legs," *IEEE Robotics and Automation Letters*, vol. 4, no. 2, pp. 1676–1683, 2019.

[11] D. A. Kurek and H. H. Asada, "The MantisBot: Design and impedance control of supernumerary robotic limbs for near-ground work," in *2017 IEEE International Conference on Robotics and Automation (ICRA)*, 2017, pp. 5942–5947.

[12] F. Parietti and H. Asada, "Supernumerary robotic limbs for human body support," *IEEE Transactions on Robotics*, vol. 32, no. 2, pp. 301–311, 2016.

[13] J. Luo, Z. Gong, Y. Su, L. Ruan, Y. Zhao, H. H. Asada, and C. Fu, "Modeling and balance control of supernumerary robotic limb for overhead tasks," *IEEE Robotics and Automation Letters*, vol. 6, no. 2, pp. 4125–4132, 2021.

[14] D. Lemus, A. Berry, S. Jabeen, C. Jayaraman, K. Hohl, F. C. T. van der Helm, A. Jayaraman, and H. Vallery, "Controller synthesis and clinical exploration of wearable gyroscopic actuators to support human balance," *Scientific Reports*, vol. 10, p. 10412, 12 2020.

[15] A. Maekawa, K. Kawamura, and M. Inami, "Dynamic assistance for human balancing with inertia of a wearable robotic appendage," in *2020 IEEE/RSJ International Conference on Intelligent Robots and Systems (IROS)*, 2020, pp. 4077–4082.

[16] J. H. Meuleman, E. H. van Asseldonk, and H. van der Kooij, "The effect of directional inertias added to pelvis and ankle on gait," *Journal of NeuroEngineering and Rehabilitation*, vol. 10, p. 40, 2013.

[17] T. Insperger, "On the Approximation of Delayed Systems by Taylor Series Expansion," *Journal of Computational and Nonlinear Dynamics*, vol. 10, no. 2, 03 2015, 024503.

[18] E. A. Butcher and O. A. Bobrenkov, "On the Chebyshev spectral continuous time approximation for constant and periodic delay differential equations," *Communications in Nonlinear Science and Numerical Simulation*, vol. 16, no. 3, pp. 1541–1554, 2011.

[19] L. Wang, *Model predictive control system design and implementation using MATLAB®*. Springer Science & Business Media, 2009.

[20] A. Wolf, J. B. Swift, H. L. Swinney, and J. A. Vastano, "Determining Lyapunov exponents from a time series," *Physica D: Nonlinear Phenomena*, vol. 16, no. 3, pp. 285–317, 1985.

[21] S. Abeywardena, E. Anwar, S. Miller, and I. Farkhatdinov, "Human balance augmentation via a supernumerary robotic tail," in *2022 44th Annual International Conference of the IEEE Engineering in Medicine & Biology Society (EMBC)*, 2022, pp. 2878–2881.

[22] ——, "Mechanical characterisation of supernumerary robotic tails for human balance augmentation," *Journal of Mechanisms and Robotics*, in press.